

On improvement of the axial-vector current with stabilised Wilson fermions

P. Fritzschn^a, J. Heitger^b and J. T. Kuhlmann^{b,*}

^a*School of Mathematics, Trinity College, College Green, Dublin, Ireland*

^b*Institut für Theoretische Physik, Westfälische Wilhelms-Universität Münster,
Wilhelm-Klemm-Straße 9, 48149 Münster, Germany*

*E-mail: fritzscp@tcd.ie, heitger@uni-muenster.de,
j.kuhlmann@uni-muenster.de*

We report on the determination of the improvement coefficient c_A for the non-singlet axial-vector current $A_\mu^a(x)$ in the framework of stabilised Wilson-Clover fermions within three flavour lattice QCD. This is done by requiring the PCAC relation to hold for two different pseudo-scalar states. To generate these states, wavefunctions altering spatial structures on the boundaries of a Schrödinger functional lattice are employed and some variations of the (previously applied) wavefunction method are explored. The improvement coefficient is determined on a few ensembles for a range of gauge couplings that is potentially useful for future applications. Preliminary results on the renormalisation constants Z_V for the vector current and Z_A for the axial-vector current are also presented.

*The 39th International Symposium on Lattice Field Theory (Lattice2022),
8-13 August, 2022
Bonn, Germany*

*Speaker

1. Introduction

Leptonic pseudo-scalar hadronic decays have a significant impact on precisely estimated entries of the CKM matrix and therefore are of great interest for indirect tests of the Standard Model. Since these decays involve the QCD hadronic matrix element of the axial-vector current

$$\langle 0 | A_\mu^a(x) | \pi^b(p) \rangle = -i p_\mu f_\pi \delta^{ab} e^{-i p x}, \quad (1)$$

lattice QCD is the favoured way to reliably estimate the low-energy part of the theory contribution to these tests.

As is well-known, Wilson fermions, while having many advantages, break chiral symmetry and need to be improved to remove its leading $O(a)$ discretisation errors. For this purpose, resorting to the well-established Symanzik improvement programme [1], the fermion action receives an extra term known as the Sheikholeslami-Wohlert term. Quark bilinears also need to be improved by adding suitable extra terms. Within this programme it turns out that the improvement term of the axial-vector current is proportional to the derivative of the pseudo-scalar density. In a mass independent scheme, the (multiplicatively) renormalised and improved current for degenerate quarks is of the form

$$(A_R)_\mu^a(x) = Z_A(1 + b_A m_q)(A_I)_\mu^a(x) = Z_A(1 + b_A m_q) [A_\mu^a(x) + c_A \partial_\mu P^a(x)] \quad (2)$$

with the axial-vector current and pseudo-scalar density being defined as

$$A_\mu^a(x) = \bar{\psi}(x) \gamma_\mu \gamma_5 \frac{\lambda^a}{2} \psi(x) \quad \text{and} \quad P^a = \bar{\psi}(x) \gamma_5 \frac{\lambda^a}{2} \psi(x). \quad (3)$$

In practice, for a non-perturbative determination of c_A and Z_A one works in the chiral limit of vanishing quark masses where the b_A -term vanishes.

Here we report on our efforts to improve and renormalise the axial-vector current for three-flavour lattice QCD with stabilised Wilson fermions (SWF) [2]. For this computation we employ ensembles with fairly large volumes ($L \approx 3$ fm), Schrödinger functional boundary conditions and lattice constants in a range between $a = 0.12$ fm ($\beta = 3.685$) and $a = 0.055$ fm ($\beta = 4.10$) in the chiral limit as well as at the symmetric point of fully degenerate sea and valence quark masses. Since SWF provide a new $O(a)$ discretisation of QCD, their improvement coefficients and renormalisation constants differ from the known $N_f = 3$ values (see e.g. [3–6]) for ordinary Wilson-Clover fermions with the same, tree-level Symanzik-improved gauge action.

2. Stabilised Wilson formulation

Numerical simulations with the Wilson-Clover Dirac operator

$$D_W = \frac{1}{2} \left\{ \gamma_\mu \left(\nabla_\mu^* + \nabla_\mu \right) - \nabla_\mu^* \nabla_\mu \right\} + c_{sw} \frac{i}{4} \sigma_{\mu\nu} F_{\mu\nu} + m_0 \quad (4)$$

require stabilising measures as proposed in [2]. Based on the observation that the clover term in D_W hinders stable inversion of the Dirac matrix, an alternative form of the Dirac operator was introduced, in which the on-site terms are exponentiated, i.e.

$$M_0 + c_{sw} \frac{i}{4} \sigma_{\mu\nu} F_{\mu\nu} \quad \rightarrow \quad M_0 \exp \left(\frac{c_{sw}}{M_0} \frac{i}{4} \sigma_{\mu\nu} F_{\mu\nu} \right), \quad (5)$$

with $M_0 = m_0 + 4$. The exponential ensures an intrinsic bound from below in this term. As a consequence, the Dirac operator does receive fewer near-zero eigenvalues, stabilising the calculation. This approach was originally developed for master-field simulations [2], but it turns out to also be beneficial for light quarks, coarse gauge fields and large lattices [7]. This is the situation we are focussing on.

While the Sheikholeslami-Wohlert coefficient c_{sw} for the new action has already been determined for a range of couplings [2, 7], the improvement coefficients for quark-bilinears such as the axial-vector current are yet to be computed.

3. Improvement of the axial-vector current

Along the lines of [4, 8], using the Schrödinger functional framework, one can derive an expression for the coefficient c_A . To do so, we introduce the correlation functions

$$f_A(x_0; \omega) = -\frac{a^3}{3L^6} \sum_{\vec{x}} \langle A_0^a(x) O^a(\omega) \rangle \quad \text{and} \quad f_P(x_0; \omega) = -\frac{a^3}{3L^6} \sum_{\vec{x}} \langle P^a(x) O^a(\omega) \rangle \quad (6)$$

with the boundary source operator at $x_0 = 0$ being defined as

$$O^e(\omega) = a^6 \sum_{\vec{y}, \vec{z}} \bar{\zeta}(\vec{y}) \gamma_5 \frac{\lambda^e}{2} \omega(\vec{y} - \vec{z}) \zeta(\vec{z}), \quad (7)$$

where ζ is the boundary quark field. Similar correlation functions can also be introduced with sources at $x_0 = T$. These are built from boundary operators $O'^f(\omega)$ and complementary boundary quark fields ζ' . In this context, ω denotes an arbitrary spatial structure on the boundary that we will call wavefunction. The first step in our analysis is to find suitable wavefunctions such that the ground and first excited state can be readily extracted from the correlators. These are approximated as in [4, 8] by constructing linear combinations of basis wavefunctions. Here we consider a set of five functions of the form

$$\omega^{\text{b1}} = e^{-\frac{r}{a_0}}, \quad \omega^{\text{b2}} = r e^{-\frac{r}{a_0}}, \quad \omega^{\text{b3}} = e^{-\frac{r}{2a_0}}, \quad \omega^{\text{b4}} = \text{const}, \quad \omega^{\text{b5}} = r^2 e^{-\frac{r}{a_0}}, \quad (8)$$

which resemble those of the hydrogen atom, with $r = |\vec{x} - \vec{y}|$ and a_0 parametrising the spatial extent of the function. To find a well-suited linear combination, the boundary-to-boundary correlator,

$$F_1(\omega^{\text{bi}}, \omega^{\text{bj}}) = -\frac{1}{3L^6} \langle O'^a(\omega^{\text{bj}}) O^a(\omega^{\text{bi}}) \rangle, \quad (9)$$

which for our purposes can be viewed as a 5×5 -matrix in wavefunction space, is evaluated. We can pick any subset of indices as a submatrix¹ and calculate its eigenvectors, sorted by eigenvalue. The „standard“ choice that was previously used in refs. [4, 8] can be regained by setting $i, j \in \{1, 2, 3\}$. In our setup it turned out that with this choice c_A inherits some ambiguity that may be avoided by other linear combinations. Hence we also explored the submatrix with $i, j \in \{1, 2, 4\}$. Exploiting the overlap information of the basis wavefunctions to approximately prepare the ground and first

¹These need to be at least 3×3 -submatrices for the eigenvectors to be fully independent of each other.

excited state then amounts to projecting the correlators f_A and f_P with given basis wavefunctions onto the eigenvectors belonging to the largest two eigenvalues.

The improvement coefficient c_A is determined in the following way: The starting point is the PCAC relation

$$\partial_\mu \langle A_\mu^a(x) O^a \rangle = 2m_{\text{PCAC}} \langle P^a(x) O^a \rangle, \quad (10)$$

which follows from an invariance under chiral rotation and holds as an operator identity in the continuum theory. Therefore, all effects that break it on the lattice must stem from the discretisation. Requiring the identity to be satisfied up to $O(a^2)$ cut-off effects amounts to inserting the improved current from eq. (2) into this relation and thus yields for the $O(a)$ improved PCAC quark mass

$$am_{\text{PCAC}} \equiv \frac{a \partial_\mu \langle (A_1)_\mu^a(x) O^a \rangle}{2 \langle P^a(x) O^a \rangle} + O(a^2), \quad (11)$$

provided c_A is fixed non-perturbatively. As detailed in the previous works, it can be rewritten in terms of the Schrödinger functional correlation functions from above as

$$a m_{\text{PCAC}}(x_0; \omega^i) = \frac{a \hat{\partial}_0 f_A(x_0; \omega^i) + c_A a^2 \hat{\partial}_0^2 f_P(x_0; \omega^i)}{2 f_P(x_0; \omega^i)}. \quad (12)$$

Decomposing the PCAC mass as

$$m_{\text{PCAC}}(x_0; \omega^i) = r(x_0; \omega^i) + c_A a s(x_0; \omega^i), \quad (13)$$

with

$$r(x_0; \omega^i) = \frac{\hat{\partial}_0 f_A(x_0; \omega^i)}{2 f_P(x_0; \omega^i)} \quad \text{and} \quad s(x_0; \omega^i) = \frac{\hat{\partial}_0^2 f_P(x_0; \omega^i)}{2 f_P(x_0; \omega^i)}, \quad (14)$$

and assuming that it holds for the two lowest states in the pseudo-scalar channel (isolated as described above) labelled by indices $i = 0, 1$, we can solve for c_A :

$$c_A(x_0) = -\frac{r(x_0; \omega^1) - r(x_0; \omega^0)}{a (s(x_0; \omega^1) - s(x_0; \omega^0))} = -\frac{\Delta r(x_0)}{a \Delta s(x_0)}. \quad (15)$$

Note that, as observed in [4, 8], the precision of the estimate for c_A is dominated by the statistical error of $a\Delta s$. Therefore an examination of the x_0 -dependence of the functions Δr and $a\Delta s$ may be helpful. As one expects $c_A(x_0)$ in eq. (15) to develop a plateau over a certain range of x_0 , a suitable plateau range needs to be identified, in which the noise in Δr and $a\Delta s$ is small.

4. Renormalisation

For the calculation of the renormalisation factor Z_A we adopt the strategy explained in [5, 9]. We only recall here that the calculation involves a Ward identity originating from an infinitesimal chiral rotation of the fields entering the expectation value

$$\langle A_v^b(y) O_{\text{ext}} \rangle = \int \mathcal{D}[\bar{\psi}, \psi, U] A_v^b(y) O_{\text{ext}} e^{-S}, \quad (16)$$

where we include the current into the chiral rotation and obtain from the variational principle

$$0 = \langle \delta A_v^b(y) O_{\text{ext}} \rangle - \langle \delta S A_v^b(y) O_{\text{ext}} \rangle. \quad (17)$$

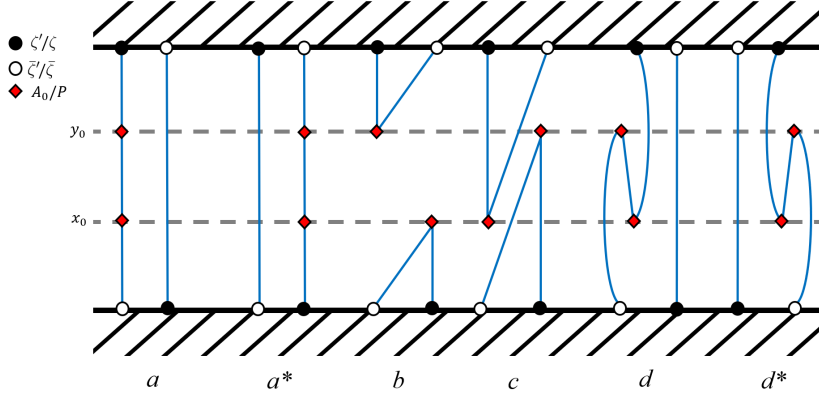


Figure 1: The six non-vanishing Wick contractions contributing to the 4-point functions F_{XY} .

For O_{ext} which we set

$$O_{\text{ext}} = O_{\text{ext}}^{ef} = O^e (O')^f, \quad (18)$$

where O^e and $(O')^f$ are the pseudo-scalar boundary sources as defined in eq. (7).

Omitting all intermediate steps, translating the expressions into their lattice counterparts and formulating them in terms of renormalised, improved Schrödinger functional correlators, one can finally isolate Z_A as

$$Z_A = \sqrt{\frac{F_1}{F_{AA}^1(x_0, y_0) - 2m_{\text{PCAC}} \tilde{F}_{PA}^1(x_0, y_0)}}, \quad (19)$$

where F_{AA}^1 is defined as

$$F_{AA}^1 = F_{AA}(x_0, y_0) + ac_A (\partial_{x_0} F_{PA}(x_0, y_0) + \partial_{y_0} F_{AP}(x_0, y_0)) + a^2 c_A^2 (\partial_{x_0} \partial_{y_0} F_{PP}(x_0, y_0)) \quad (20)$$

and \tilde{F}_{PA}^1 as

$$\tilde{F}_{PA}^1(x_0, y_0) = \tilde{F}_{PA}(x_0, y_0) + c_A \partial_{y_0} \tilde{F}_{PP}(x_0, y_0), \quad (21)$$

with

$$F_{XY}(x_0, y_0) \equiv -2a^6 \sum_{\vec{x}, \vec{y}} \langle X^1(x) Y^2(y) O^2(O')^1 \rangle \quad (22)$$

and

$$\tilde{F}_{XY}(x_0, y_0) \equiv a \sum_{z_0=x_0}^{y_0} w(z_0) F_{XY}(z_0, y_0) \quad \text{with} \quad w(z_0) = \begin{cases} \frac{1}{2} & \text{if } z_0 = x_0 \text{ or } z_0 = y_0 \\ 1 & \text{else} \end{cases}. \quad (23)$$

Each of the 4-point functions receives contributions from six different diagrams shown in fig. 1. Two of these are disconnected and can be evaluated as a product of two separate 2-point functions.

Additionally, in this calculation we consider the vector current which enters the following Ward identity:

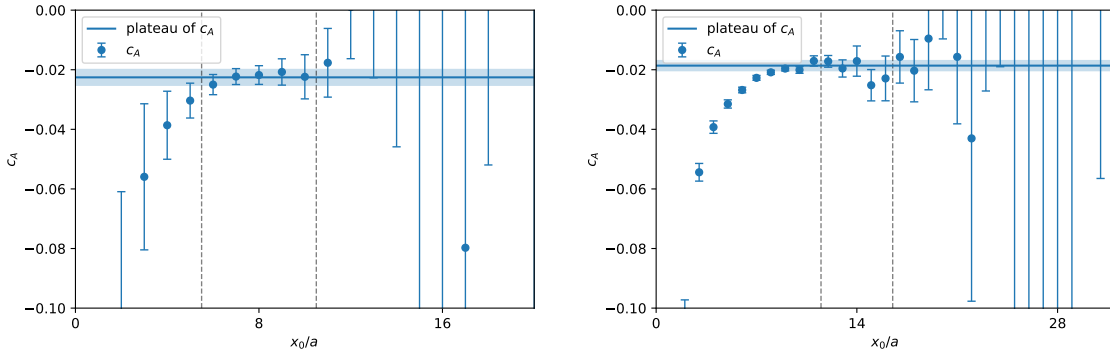
$$\int d^3y \langle V_0^c(y) O^e(O')^f \rangle = i f_g^{ce} \langle O^g(O')^f \rangle, \quad (24)$$

where O^e and $(O')^f$ are defined as before. From this, a simple expression for Z_V can be derived [10]:

$$Z_V = \frac{F_1}{f_V} + O(a^2), \quad (25)$$

Table 1: Ensembles with Schrödinger functional boundary conditions used in this project. The mass point indicates to which line of constant physics the ensemble belongs.

T	L^3	β	$\kappa_{u/d/s}$	a [fm]	mass point	# of configs
24	16^3	3.80	0.1392500	0.095	chir.	2875
24	24^3	3.80	0.1392500	0.095	chir.	2523
32	32^3	3.80	0.1392500	0.095	chir.	1167
24	24^3	3.685	0.1394400	0.120	symm.	540
32	32^3	3.80	0.1389630	0.095	symm.	956
56	56^3	4.10	0.1380000	0.055	symm.	33

**Figure 2:** Preliminary results for c_A at $\beta = 3.80$ ($a \approx 0.094$ fm, left) at the chiral point and $\beta = 4.10$ ($a \approx 0.055$ fm, right) at the symmetric point with the standard projection.

in which f_V is

$$f_V(x_0) = i \sum_x \varepsilon_{abc} \langle O'^a V_0^b(x_0) O^c \rangle. \quad (26)$$

5. Ensembles and error analysis

After having discussed the theoretical aspects, we introduce the ensembles used in the numerical computations so far. To make our results on c_A , Z_A and Z_V useful for other groups, the range of ensembles covered are at the same lattice spacings a as those generated by OpenLat² [7], only differing in boundary conditions. The ensembles used here are listed in tab. 1. Our error analysis is done employing the Γ -method [11] using the python-implementation pyerrors described in [12]. As stated in the introduction, we are interested in two lines of constant physics: at the chiral point of (almost) vanishing quark masses and at the symmetric point of fully degenerate massive quark flavours.

6. Results

In the analysis for c_A we have seen that the quality and longevity of the plateau may be problematic in the large-volume setup adopted here. For the preliminary results we set the plateau

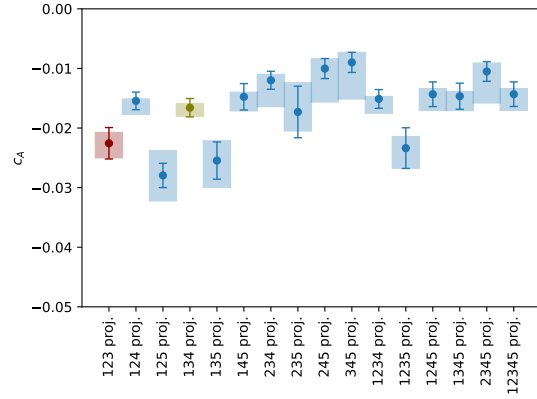
²see also: <https://openlat1.gitlab.io/>

Table 2: Preliminary estimates of renormalisation constants for the axial-vector channel. The labels f, c and m refer to full, connected and massive definitions of Z_A ; see [5] for details.

Ensemble	Z_A^f	$Z_A^{f,m}$	Z_A^c	$Z_A^{c,m}$
24×16^3 , $\beta = 3.80$, chir.	0.7638(76)	0.7585(80)	0.753(20)	0.773(21)
24×24^3 , $\beta = 3.80$, chir.	0.779(15)	0.741(13)	0.7631(50)	0.7782(39)

region as $x_0 \in [T/4 - 2, T/4 + 2]$, which works out fine in most cases, as can be seen for the two representative examples in fig. 2.

As mentioned above, it has also been seen in our tests that the standard projection (used in [4, 8]) is not always optimal. An alternative was found by scanning all possible projections which can be built after diagonalising F_1 on various (subsets of) basis wavefunctions. The outcome of these scans can be inferred from fig. 3. While the standard projection shown in red, assessed in isolation, yields a legitimate value, the majority of the other projections are placed systematically around a different value. This could hint at an overestimation of c_A (in magnitude) when using the standard projection. However, the new, preferred projection exhibits smaller errors and yields results consistent with most other projections, thus appearing to be less affected by systematics due to the choice of the wavefunction basis. The spread of c_A in the plateau region (shown in fig. 3 by the vertical extent of the boxes) is also smaller for this projection, which endorses the better quality of the associated plateau.


Figure 3: Example for the possible projections on the 32^4 lattice at $\beta = 3.80$ at the chiral point. Data points shown here are the plateau-values of $x_0 \in [T/4 - 2, T/4 + 2]$. The boxes indicate the spread of c_A in the plateau region. The standard projection is marked in red, while the new, preferred projection is marked in green.

In fig. 4 a preliminary interpolation in g_0^2 of the results on the symmetric point ensembles is displayed. So far, the ensembles studied do not yet allow for an analogous interpolation in the chiral case. However, we can see that in comparison with the results for ordinary Wilson-Clover fermions [4] the estimates for c_A appear to be smaller in magnitude which may hint at smaller cut-off effects for stabilised Wilson fermions at the same lattice spacing. Of course, whether this is a general feature of this discretisation still needs to be confirmed in phenomenological applications.

For the renormalisation constants, preliminary results are listed in tables. 2 and 3. These indicate that the estimates obtained are within the same ballpark as the ones for ordinary Wilson-Clover fermions in $N_f = 3$ [5, 13]. As the 4-point functions used here are prone to large statistical fluctuations, it seems more promising to determine Z_A in the chirally rotated Schrödinger functional (χ SF) scheme [6, 14], because in this framework only 2-point functions are involved.

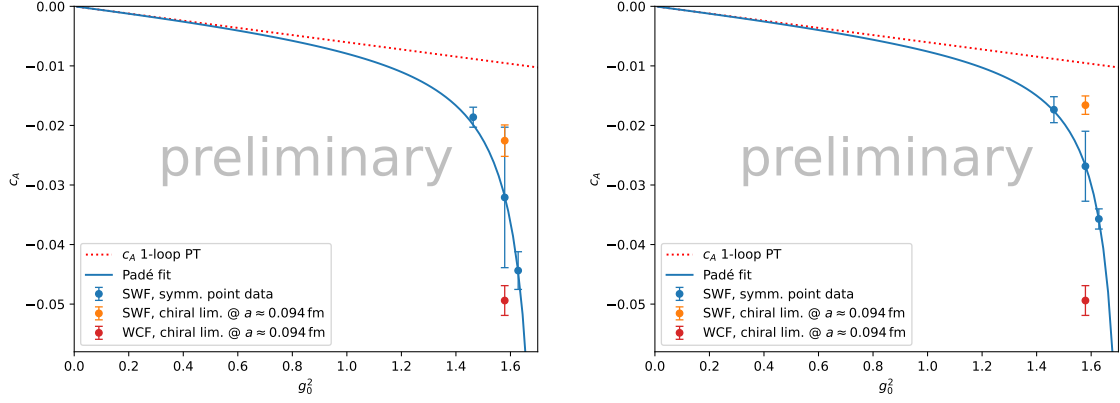


Figure 4: Preliminary g_0^2 -dependence of c_A for ensembles at the symmetric point with $\beta = 3.685$, $\beta = 3.80$, $\beta = 4.10$ with the standard (left) and the preferred (right) projection. In orange, the point for the chiral case at $\beta = 3.80$ is shown. The red point gives $N_f = 3$ result for traditional Wilson-Clover fermions from [4].

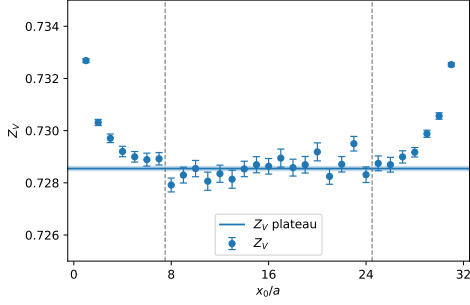


Figure 5: Example for the calculation of Z_V on the chiral ensemble at $\beta = 3.80$ ($a \approx 0.094$ fm).

Table 3: Preliminary estimates of renormalisation constants for the vector channel.

Ensemble	Z_V
24×16^3 , $\beta = 3.80$, chir.	0.729141(94)
24×24^3 , $\beta = 3.80$, chir.	0.728716(56)
32×32^3 , $\beta = 3.80$, chir.	0.728546(81)
24×24^3 , $\beta = 3.685$, symm.	0.71209(13)
32×32^3 , $\beta = 3.80$, symm.	0.738044(53)
56×56^3 , $\beta = 4.10$, symm.	0.777900(17)

The values for Z_V in tab. 3 were extracted from plateau ranges like the one shown in fig. 5. Due to the simple expression for Z_V in eq. (25), which only consists of a ratio of two correlation functions and yields a good plateau quality in most cases, it can be determined to high precision. In the present, preliminary results, plateaus have been taken from $x_0 = T/4$ up to $x_0 = 3T/4$.

7. Conclusions and outlook

We have seen that the Ward identity method in combination with Schrödinger functional boundary conditions can be readily implemented to determine c_A for the stabilised Wilson-Clover fermions. As we work in larger volumes, some adaptations in the choice of the plateau range and wavefunctions turn out to be advantageous to reach the desired precision goal. To finally arrive at a proper interpolation over the whole range of interesting lattice spacings, measurements on further ensembles are still to be added.

When it comes to renormalisation, a precise extraction of Z_V for the vector current is straightforward, while the achievable accuracy for Z_A remains to be seen. A promising route to enhance the final precision of Z_A is to pursue the computational strategy within the χ SF advocated and successfully applied in [6, 14].

References

- [1] M. Lüscher, S. Sint, R. Sommer, and P. Weisz, *Chiral symmetry and $O(a)$ improvement in lattice QCD*, *Nucl. Phys. B* **478** (1996) 365, [[hep-lat/9605038](#)].
- [2] A. Francis, P. Fritzsche, M. Lüscher, and A. Rago, *Master-field simulations of $O(a)$ -improved lattice QCD: Algorithms, stability and exactness*, *Comput. Phys. Commun.* **255** (2019) 107355, [[1911.04533](#)].
- [3] J. Bulava and S. Schaefer, *Improvement of $N_f = 3$ lattice QCD with Wilson fermions and tree-level improved gauge action*, *Nucl. Phys. B* **874** (2013) 188, [[1304.7093](#)].
- [4] J. Bulava, M. D. Morte, J. Heitger, and C. Wittmeier, *Non-perturbative improvement of the axial current in $N_f = 3$ lattice QCD with Wilson fermions and tree-level improved gauge action*, *Nucl. Phys. B* **896** (2015) 555, [[1502.04999](#)].
- [5] J. Bulava, M. D. Morte, J. Heitger, and C. Wittmeier, *Non-perturbative renormalization of the axial current in $N_f = 3$ lattice QCD with Wilson fermions and tree-level improved gauge action*, *Phys. Rev. D* **93** (2016) 114513, [[1604.05827](#)].
- [6] M. Dalla Brida, T. Korzec, S. Sint, and P. Vilaseca, *High precision renormalization of the flavour non-singlet Noether currents in lattice QCD with Wilson quarks*, *Eur. Phys. J. C* **79** (2019) 23, [[1808.09236](#)].
- [7] A. S. Francis, F. Cuteri, P. Fritzsche, G. Pederiva, A. Rago, A. Schindler, A. Walker-Loud, and S. Zafeiropoulos, *Properties, ensembles and hadron spectra with Stabilised Wilson Fermions*, *PoS LATTICE2021* (2022) 118, [[2201.03874](#)].
- [8] M. Della Morte, R. Hoffmann, and R. Sommer, *Non-perturbative improvement of the axial current for dynamical Wilson fermions*, *JHEP* **03** (2005) 029, [[hep-lat/0503003](#)].
- [9] M. Della Morte, R. Hoffmann, F. Knechtli, R. Sommer, and U. Wolff, *Non-perturbative renormalization of the axial current with dynamical Wilson fermions*, *JHEP* **07** (2005) 007, [[hep-lat/0505026](#)].
- [10] M. Lüscher, S. Sint, R. Sommer, P. Weisz, and U. Wolff, *Non-perturbative $O(a)$ improvement of lattice QCD*, *Nucl. Phys. B* **491** (1996) 323, [[hep-lat/9609035](#)].
- [11] U. Wolff, *Monte Carlo errors with less errors*, *Comput. Phys. Commun.* **156** (2003) 143, [[hep-lat/0306017](#)].
- [12] F. Joswig, S. Kuberski, J. T. Kuhlmann, and J. Neuendorf, *pyerrors: a python framework for error analysis of Monte Carlo data*, [2209.14371](#).
- [13] J. Heitger and F. Joswig, *The renormalised $O(a)$ improved vector current in three-flavour lattice QCD with Wilson quarks*, *Eur. Phys. J. C* **81** (2021) 254, [[2010.09539](#)].
- [14] S. Sint, *The chirally rotated Schrödinger functional with Wilson fermions and automatic $O(a)$ improvement*, *Nucl. Phys. B* **847** (2010) 491, [[1008.4857](#)].